A Mechanically Steerable Array Antenna with Controllable Microwave Phase Shifters at 20 GHz

Junho Cha and Yasuo Kuga*
Department of Electrical Engineering
University of Washington, Box 352500
Seattle, WA 98195

James T. Kajiya
Microsoft Corporation
Redmond, WA 98052

Abstract

A mechanically steerable antenna was designed and developed using an adjustable microwave phase shifter. The dielectric material $\varepsilon_r = 10$ (Alumina) was used as the dielectric slab and was placed close to a coplanar TL. Numerical simulations using Ansoft HFSS and Designer were conducted at 20 GHz. For the testing purpose, a 4-element steerable array antenna at 5.8 GHz was fabricated and measured.

I. Introduction

The design of a phase shifter has attracted much interest because of its importance in numerous applications. Phase shifters are a critical element for electronically scanned phased array antennas, and typically account for a significant amount of the cost of producing an antenna array. This newly proposed phase shifter design is anticipated to be easy to fabricate. The reduction of fabrication cost opens possibilities for many applications. It will, for instance, allow the antenna to be suitable for Low Earth Orbit (LEO) satellite systems operating at Ku-Ka bands.

To create the phase shifter, a movable dielectric slab is placed close to a coplanar waveguide (CPW). The effective dielectric constant is calculated as a function of slab height, and the characteristics of the basic 4-element array antenna (shown in Fig. 1) are simulated at 20 GHz. The preset delay is added to scan the beam from -30^0 to $+30^0$. We compare the simulated radiation patterns and the measured radiation patterns of the steerable array antenna at 5.8 GHz.

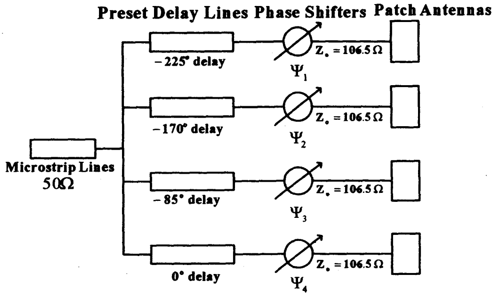

Fig. 1: Block diagram of a 4-element steerable phased-array antenna at 20 GHz.

0-7803-8883-6/05/$20.00 ©2005 IEEE

II. Proposed Phase Shifter Based on a Movable Dielectric Slab

The basic concept of the proposed phase shifter is illustrated in Fig. 2. As is demonstrated, the movable dielectric constant slab is inserted into the gap of the CPW. The effective dielectric constant is a function of *d* for a given structure. In this design, the CPW for *d*=5mm (effectively $d=\infty$) has the characteristic impedance $Z_0 = 106.5\Omega$ and the effective dielectric constant of $\varepsilon_{\text{effective}}$ = 1.425. As the distance *d* decreases, $\varepsilon_{\text{effective}}$ increases and Z_0 decreases. The modeling orchestrated for this phase shifter was conducted for height *d* from *d*=0 to *d*=5 mm. We estimated the effective dielectric constant from the S_{21} data [1].

The phase change at the slab height *d* (with respect to that without a dielectric slab ($d=\infty$)), can be expressed as

$$\theta_d = k_o L_d\left(\sqrt{\varepsilon_{eff\_d}} - \sqrt{\varepsilon_{eff\_d=\infty}}\right) \qquad (1)$$

where k_0 is the wavenumber in free space, L_d is the slab length, $\varepsilon_{eff\_d=\infty}$ is the effective dielectric constant when the dielectric material is far enough away from the substrate, and ε_{eff_d} is the effective dielectric constant at slab height *d*.

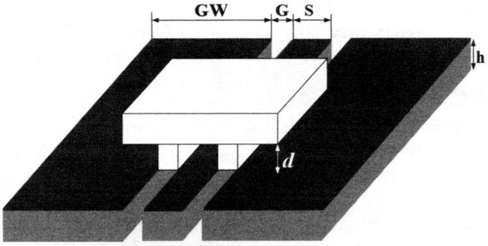

Fig. 2: Phase shifter. A 3-D schematic of a ground-signal-ground (G-S-G) CPW with a movable dielectric slab. The width of the signal trace is 2 mm and the width of the ground trace is 6 mm. The gap between the ground and the signal is 1 mm. Substrate thickness is 1.524 mm and the height of dielectric material is 2.54 mm. The length of the dielectric material is 2.6 mm, while the gap width of the dielectric material is 0.8 mm. The dielectric constant of the dielectric material is $\varepsilon_r = 10$, and the substrate has ε_{sub}=3.38 (IS 640).

III. Numerical Results

The CAD model with the slab at height *d* is shown in Fig. 2 [2]. A G-S-G TL with the center gap was found to provide a reasonable amount of phase shift with a dielectric slab. Table 1 presents numerical results for the G-S-G TL with the center gap for cases where the distance *d* is between $0 \le d \le 5$ mm from the dielectric slab.

As Table 1 demonstrates, the characteristic impedance, the effective dielectric constant, and the phase difference are changed depending on the distance of the dielectric material from the substrate. We decided on a gap width of 0.8 mm for the dielectric material instead of 1mm because it was easier to insert into the gap of the CPW. This antenna is designed to scan with the phase difference of -85^0 to $+85^0$ with an expected beam scan angle of -30^0 to $+30^0$ as shown in Fig. 1. The simulated radiation patterns conducted at 20 GHz are shown in Fig. 3. In order to remove the grating mode, the antenna separation is set to 1.5 mm which is less than $\lambda/2$.

d(mm)	Z_0	ε_{eff}	Phase difference (θ_d)
0	64	6.558	85.81^0
0.1	85	4.078	52.01^0
0.25	91.2	3.342	40.06^0
0.5	95.3	2.863	31.00^0
0.75	97.5	2.604	26.68^0
1	99.2	2.403	22.71^0
1.25	100.9	2.198	18.49^0
1.5	103.2	1.919	12.41^0
2	106.2	1.545	3.53^0
3	106.3	1.430	NA
4	106.4	1.428	NA
5	106.5	1.425	NA
Air	106.5	1.524	NA

Table 1: Simulated results from *d*=0 mm to *d*=5mm at 20 GHz.

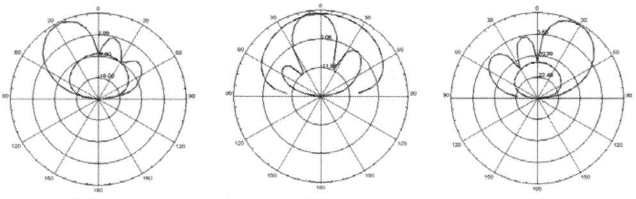
(a) (b) (c)

Fig. 3: Radiation patterns of a 4-element array antenna (from Fig. 1) at 20 GHz (a): The pattern resulting when the dielectric slab is attached to the substrate (*d*=0 mm). (b): The pattern resulting when the dielectric slab is 0.25 mm above the substrate (*d*=0.25 mm). (c): The pattern resulting when the dielectric slab is far from the substrate (*d*=5 mm). In these cases, the width of the patch is 5.8 mm and the height of the patch is 3.16 mm. The element separation is 1.5 mm while the input impedance is 106.5Ω.

IV. Fabrication of a 4-element steerable array antenna at 5.8 GHz

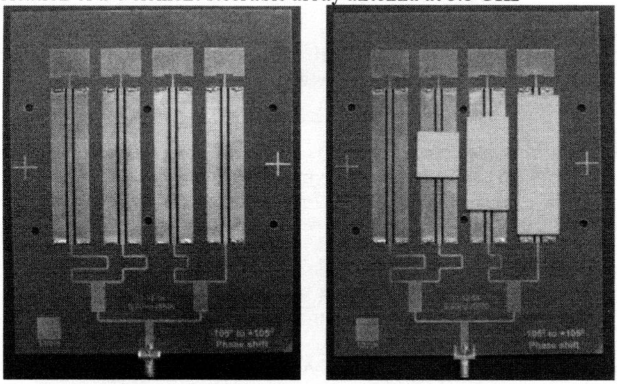
Fig. 4: Fabrication of a 4-element array antenna

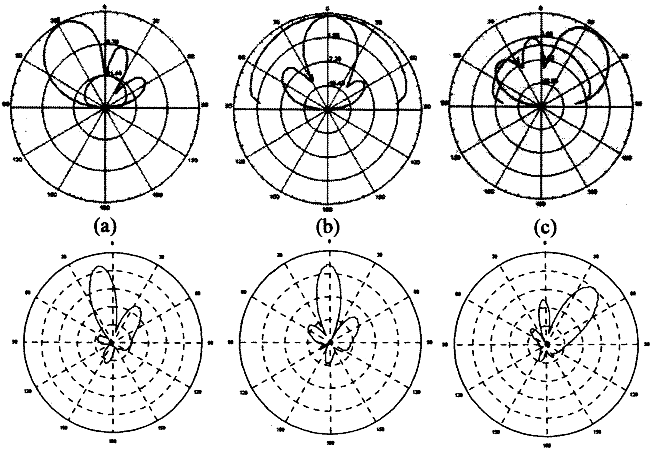

(a) (b) (c)

(d) (e) (f)

Fig. 5: Simulated and measured radiation patterns at 5.8 GHz. The top figures (a,b,c) are the simulated radiation patterns (from Fig. 4) while the bottom figures (d,e,f) are the measured radiation patterns. (a) and (d) represent patterns when the dielectric slab is attached to the substrate (*d*=0 mm). (b) and (e) occur when the dielectric slab is 0.1 mm above the substrate (*d*=0.1 mm). (c) and (f) represent patterns when the dielectric slab is far from the substrate (*d*=5 mm).

To demonstrate the feasibility of our concept, the 4-element steerable array antenna was designed and fabricated at 5.8 GHz. An additional benefit of testing at 5.8 GHz is the potential use for the wireless network. The test antenna is designed to scan with a phase difference of -105^0 to $+105^0$. In Fig. 4, preset delay lines of -105^0, -210^0, and -315^0 correspond to the phase delay while the dielectric slabs represent -210^0, -420^0, and -630^0 phase change, respectively. The dielectric constant of the dielectric material is $\varepsilon_r=10$ and the height of the dielectric material is 5 mm. In Fig. 5, the simulated and the measured radiation patterns were compared. As it turns out, the expected radiation patterns and measured radiation patterns are quite similar. However, the radiation patterns of (a) and (d) show substantial difference. This discrepancy seems to be due to a small residual gap (less than 10 μm) between the dielectric slab and conductors.

V. Conclusions

A mechanically steerable array antenna was proposed. The proposed antenna was tested at 5.8 GHz. Although the TL impedance is matched at $d=0$ and $d \geq 2$ mm, the impedance mismatch can be a problem between $0<d<2$ mm. The next step is to fabricate a steerable array antenna at 20 GHz.

References

1. Y. Kuga, J. Cha, J. A. Ritcey, and J. T. Kajiya, "Mechanically Steerable Antenna Using Dielectric Phase Shifters," 2004 IEEE AP-S International Symposium, vol. 1, pp. 161-164, June 20-26, Monterey, CA.
2. J. Cha, Y. Kuga, and S. Lee, "A Phased-Array Antenna with Mechanically Controllable Microwave Phase Shifters," URSI 2005, pp. 60, Jan. 2005, Boulder, CO.